INTELLIGENT BUILDING THERMAL ENERGY MANAGEMENT SYSTEM BASED ON MULTI-SOURCE DATA FUSION
Heat Flow Prediction and Scheduling Based on IoT and Deep Learning

by

Youpeng HUANG *

Beijing Institute of Economics and Management, Beijing, China

Original scientific paper
https://doi.org/10.2298/TSCI2506207H

This paper studies the intelligent building thermal energy management system based on multi-source data fusion, explores the multi-source fusion method suitable for building thermal energy data, constructs an improved LSTM-CNN fusion model based on attention mechanism, formulates a thermal energy scheduling strategy based on heat flow prediction, and verifies the effectiveness of the system through experiments. The experiment uses the annual monitoring data of a smart office building and the relevant benchmark data set in the USA. The results show that the RMSE of the improved model for winter heat flow prediction is as low as 0.72 ℃, which is 21.3% lower than the traditional LSTM. The scheduling strategy achieves a 14.3% reduction in daily average energy consumption, the temperature compliance rate reaches 96.8%, and the system average response time is 0.8 second, which meets the real-time requirements and provides strong support for the efficient management of thermal energy in intelligent buildings.

Key words: *multi-source data fusion, intelligent building, dynamic scheduling, thermal energy management, deep learning, heat flow prediction, IoT*

Introduction

With the continuous advancement of urbanization and the ongoing improvement in building intelligence, the proportion of intelligent buildings in total energy consumption is increasing year by year. The thermal energy management link largely determines the overall energy consumption of the building. The previous thermal energy management mode often relies on manual experience judgment or simple automatic control means [1]. When dealing with dynamically changing environments and real-time needs of users, it usually responds slowly, and the control accuracy of energy consumption is relatively low. At the same time, the building thermal energy system covers multiple operating links and various types of equipment [2]. The data generated is not only huge in quantity, but also very complex in type. How to efficiently integrate these data to provide strong support for accurate heat flow prediction and scheduling has become an urgent task facing the current intelligent building field. The development of IoT technology has made the real-time collection of multi-source data a reality [3]. The advantages of deep learning in processing non-linear and high dimensional data have created conditions for improving the accuracy of heat flow prediction. Therefore, research on intelligent building thermal energy management systems with multi-source data fusion has significant practical value.

* Author's e-mail: youpenghuang@biem.edu.cn

In the field of intelligent building thermal energy management, although some relatively mature systems have been developed abroad, there is still a lot of room for improvement in the deep application of multi-source data fusion. Domestic related research and exploration still needs to be further improved in the accuracy of heat flow prediction and the dynamic adjustment ability of scheduling strategies [4]. In the field of multi-source data fusion, existing fusion methods struggle to strike a balance between speed and accuracy. In terms of heat flow prediction and scheduling, traditional prediction methods, such as time series analysis and regression analysis, are not ideal for complex and variable heat flow characteristics. The LSTM, CNN, and other deep learning methods have been gradually applied to this field. The LSTM performs well in processing time series data, and CNN has certain advantages in extracting spatial features. Still, a single model has obvious limitations in capturing the spatiotemporal coupling characteristics of heat flow. Additionally, most existing scheduling strategies are based on static models, which are challenging to adapt to real-time changes in heat flow demand. Traditional rule-based scheduling has winter heat flow prediction RMSE >1.2 ℃ (66% higher than our model) and 15%-20% energy waste due to delayed responses to occupancy/weather changes.

The research work of this paper mainly includes: first, exploring the multi-source fusion method applicable to building thermal energy data to improve the quality of data, second, constructing a heat flow prediction model based on deep learning to enhance the accuracy of heat flow prediction, third, formulating a heat energy scheduling strategy based on the heat flow prediction results to achieve optimal energy allocation; fourth, verifying the effectiveness and superiority of the proposed system through experimental simulation [5].

Construction of heat flow prediction model based on deep learning

Model selection and improvement

Existing deep learning models have limitations in predicting heat flow. The LSTM can capture the long-term dependence of time series, but it is not sensitive to spatial features. The CNN is good at extracting local spatial features, but it struggles to handle temporal dynamic changes [6]. This study innovatively designs an improved LSTM-CNN fusion model incorporating the attention mechanism to facilitate the collaborative extraction of spatiotemporal features. The model first processes the fused multi-source data through the CNN layer, and its convolution operation can be expressed as:

$$F_s(i,j) = \sigma\left[\sum_{m=1}^{3}\sum_{n=1}^{3} W_s(m,n)\, X(i+m-1, j+n-1) + b_s\right] \tag{1}$$

where $F_s(i, j)$ is the output feature of the s convolution kernel, W_s – the convolution weight, X – the input data, b_s – the bias term, and σ – the uses the improved Leaky-ReLU activation function $\sigma(x) = \max(0.1x, x)$ to enhance the expression of feature sparsity. To solve the problem of traditional pooling losing key information, an adaptive pooling formula is designed:

$$P(i,j) = \max_{k,l}\left[F(i+k, j+l)\,\alpha_{k,l}\right] \tag{2}$$

where $\alpha_{k,1}$ is the spatial attention weight, which is dynamically generated by the sigmoid function make the pooling process focus on the high contribution area. The $\alpha_{k,1} = \text{sigmoid}(W_a F_{k,1} + b_a)$, calibrated via 10000 samples to focus on 3×3 high gradient regions (*e.g.*, morning peaks). This reduces feature loss by 40% *vs.* standard max pooling.

Model structure design

The model input is the fused 3-D tensor (N, T, F), where N is the number of samples, T = 1440 (minute-level time step), and F is the feature dimension (including 18 types of features such as environment, equipment, and user behavior).

The CNN module adopts a dual-channel parallel structure. The first channel extracts local features through $64 \times 3 \times 3$ convolution kernels, and the second channel uses $16 \times 7 \times 7$ convolution kernels to capture global spatial associations. The feature fusion formula:

$$F_{\text{cnn}} = \text{Concat}\left(F_{3\times3}, F_{7\times7}\right)M \tag{3}$$

where $M \in R^{160\times96}$ is the learnable fusion matrix that realizes adaptive compression of feature dimensions. The $M \in R^{160\times96}$ merges $64 \times 3 \times 3 + 16 \times 7 \times 7$ features (160 channels total) into 96, reducing dimensionality by 40% while retaining 95% variance, validated via PCA.

The LSTM module introduces a gate improvement mechanism, and the calculation formula of the forget gate is:

$$f_t = \sigma\left(W_f\left[h_{t-1}, x_t\right] + b_f + \gamma\frac{1}{T}\sum_{k=1}^{T}h_k\right) \tag{4}$$

The newly added term:

$$\gamma\frac{1}{T}\sum_{k=1}^{T}h_k$$

dynamically adjusts the forgetting strength through the historical hidden state mean, and γ is the adjustment coefficient. The γ = 0.3 was tuned via grid search (0.1-0.5) to minimize validation loss. Higher γ (0.5) causes overfitting to recent data. Lower (0.1) weakens long-term memory.

The attention module uses the second-order interaction weight calculation:

$$\alpha_t = \frac{\exp\left(q_t K^T V_t\right)}{\sum_{k=1}^{T}\exp\left(q_k K^T V_k\right)} \tag{5}$$

where q_t is the query vector and K, V are the key matrix and value matrix, respectively, and the weight allocation accuracy is improved by capturing the second-order association between features. The final fully connected layer outputs the predicted heat flow value:

$$\hat{Q} = \sum_{t=1}^{T}\alpha_t h_t W_o + b_o,\ W_o,\ b_o$$

are output layer parameters.

Model training and optimization

The data set is divided into 7:1:2 and contains 12 months of monitoring data of 3 buildings (a total of 86400 samples). The training uses a mixed loss function:

$$L = \lambda_1 RMSE + \lambda_2 MAE + \lambda_3 \text{MaxAE} \tag{6}$$

where λ_1= 0.5, λ_2 = 0.3, λ_3 = 0.2, MaxAE is the maximum absolute error, which enhances the model's ability to fit extreme values. The optimizer uses the improved Adam algorithm, and the learning rate update formula is:

$$\eta_t = \eta_0 \exp\left(-\beta \frac{\Delta L_t}{\Delta L_0}\right) \tag{7}$$

where $\beta = 0.02$, L_t is the current validation loss change rate, which realizes adaptive non-linear adjustment of learning rate. Regularization adopts a hybrid strategy: in addition L_2 regularization (coefficient 0.001), the feature sparse regularization term:

$$L_{\text{sparse}} = \sum_{f=1}^{F} \log\left(1 + \left|w_f\right|\right)$$

is introduced to suppress the influence of redundant features. The training process adopts a dynamic batch processing strategy. When the loss reduction rate is <5%, the batch size automatically increases from 32 to 64 to balance training efficiency and stability. The gradient distribution and feature importance weights are monitored in real time through TensorBoard. When the standard deviation of the feature weight is <0.01, the parameter fine-tuning mechanism is triggered to ensure continuous optimization of the model.

Thermal energy scheduling strategy based on heat flow prediction

Scheduling objectives and constraints

Thermal energy scheduling is centered on the dual-objective optimization of *comfort – energy consumption*, minimizing energy consumption while ensuring that the indoor temperature remains within the comfortable range of 22-26 °C. The setting of this goal considers both the user's physical needs and the energy-saving benefits of the building, and is key to balancing user experience and sustainable development. To accurately quantify the comfort constraint, a temperature deviation penalty function is constructed:

$$C(T) = \begin{cases} k_1 (T - 26)^2 & T > 26 \\ 0 & 22 \le T \le 26 \\ k_2 (22 - T)^2 & T < 22 \end{cases} \tag{8}$$

where $k_1 = 1.2$, $k_2 = 1.5$ are the asymmetric penalty coefficients, and a higher weight is set for low temperature deviation. This is because the low temperature environment has a more significant impact on the user's body and requires stricter control.

In terms of equipment constraints, the boiler heating power must meet $P_{\min} \le P(t) \le P_{\max}$ where $P_{\min}$ is the minimum safe operating power of the boiler and $P_{\max}$ is the maximum designed heating power of the boiler, ensuring that the boiler operates within a safe and efficient range. The water pump flow constraint is $Q_{\min} \le Q(t) \le Q_{\max}$, $Q_{\min}$ and $Q_{\max}$ are the minimum and maximum allowable flow rates of the water pump, respectively, to prevent the water pump from idling due to too small flow or excessive flow exceeding the pipe-line carrying capacity [7]. At the same time, the equipment start-stop state $S(t) \in \{0, 1\}$ must meet the rigid constraint of continuous operation time ≥30 minutes, to avoid losses and energy waste caused by frequent start-stop of equipment.

The pipe-line network pressure balance equation reflects the energy supply constraint:

$$\Delta P(t) = \sum_{i=1}^{n} R_i Q_i(t)^2 \le \Delta P_{\max} \tag{9}$$

where R_i is the pipe-line resistance coefficient, which is related to factors such as pipe-line material and pipe diameter and $\Delta P_{\max}$ – the maximum allowable pressure drop, which ensures that heat energy can be stably transmitted to each user area in the pipe-line network.

Construction of scheduling model

The objective function is defined as the minimum weighted sum of total energy consumption and comfort penalty within the scheduling period:

$$\min J = \omega_1 \sum_{t=1}^{T} \left[E_{\text{boiler}}(t) + E_{\text{pump}}(t) + E_{\text{loss}}(t) \right] + \omega_2 \sum_{t=1}^{T} C\left(T(t)\right) \tag{10}$$

where $\omega_1 = 0.7$, $\omega_2 = 0.3$ are weight coefficients, which are adjusted according to the building's emphasis on energy consumption and comfort in different seasons. In winter, ω_2 can be appropriately increased to ensure the heating effect, and in summer, ω_1 can be appropriately adjusted to give priority to energy saving.

Boiler energy consumption:

$$E_{\text{boiler}}(t) = P(t)\eta^{-1}\left(P(t)\right)$$

where $\eta(P)$ is a non-linear efficiency function that satisfies $\eta(P) = 0.85 - 0.001P$. This function reflects the efficiency change of the boiler under different powers. When the power is too high, the efficiency will decrease. Pump energy consumption:

$$E_{\text{pump}}(t) = k_q Q(t)^3$$

where k_q is the energy consumption coefficient, which is relaed to the pump model. Heat energy loss:

$$E_{\text{loss}}(t) = \alpha L \left[T_{\text{supply}}(t) - T_{\text{env}}(t) \right]$$

where α is the heat transfer coefficient, which is related to the thermal insulation performance of the pipe-line, L – the pipe-line length, $T_{\text{supply}}(t)$ – the water supply temperature, and $T_{\text{env}}(t)$ – the ambient temperature. This formula reflects the loss of heat energy due to temperature difference during transmission.

Introduce the heat flow balance constraint equation:

$$Q_{\text{pred}}(t) = Q_{\text{supply}}(t) - E_{\text{loss}}(t) - \sum_{i=1}^{m} Q_{\text{user},i}(t) \tag{11}$$

where $Q_{\text{pred}}(t)$ is the predicted heat flow and $Q_{\text{user},i}(t)$ – the heat demand of users in each area. This equation ensures the balance between the predicted heat flow and the actual supply, loss and user demand.

When solving with mixed integer programming, the device state $S(t)$ is set to a 0-1 variable. The 0 means the device is off, and 1 means the device is running. The logical constraints are processed by the big M method: $P(t) \le S(t)P_{\max}$, where M is a sufficiently large number. When the device is off $S(t) = 0$, $P(t)$ must be 0, which ensures the validity of the constraint.

Scheduling strategy optimization

Design dynamic correction coefficient $\delta(t)$ to achieve rolling optimization:

$$\delta(t) = 1 + \gamma \frac{\left|\epsilon(t)\right|}{\bar{\epsilon}} \exp\left(-\frac{\left|\epsilon(t) - \epsilon(t-1)\right|}{\sigma} \right) \tag{12}$$

where $\epsilon(t)$ is the prediction error, that is, the difference between the actual heat flow and the predicted heat flow, $\bar{\epsilon}$ – the error mean, σ – the error standard deviation, calculated through his-

torical data, and $\gamma = 0.15$ – the adjustment factor, the size of which determines the magnitude of the correction [8]. When the prediction error is significant and changes dramatically, the value of $\delta(t)$ will increase, thereby increasing the correction of the scheduling strategy.

When $|\epsilon(t)| > 1.2\bar{\epsilon}$, the emergency correction mechanism is triggered to adjust the heating power in real time:

$$P'(t) = P(t)\delta(t) + \lambda\left[T_{\text{set}} - T(t)\right] \tag{13}$$

where $\lambda = 0.8$ is the proportional adjustment coefficient, T_{set} – the set temperature, and $T(t)$ – the actual temperature. This formula comprehensively considers the impact of prediction error and temperature deviation on heating power, making the adjustment more in line with actual needs.

Experimental simulation and result analysis

Experimental data set and environment

The experimental data set is divided into two layers: the basic data set comes from the annual monitoring data of a 10-story smart office building, including 15 minutes interval environmental parameters (8 categories), equipment operation data (12 categories), and user behavior data (6 categories), with a total of 78420 valid samples. The supplementary data set uses the building energy consumption benchmark data set released by the Berkeley Laboratory in the USA, including five commercial buildings in three climate zones, to enhance the generalization verification of the model. Missing data (<3%) filled via KNN imputation (error <0.5 °C). Comparing imputed *vs*. complete subsets showed <1% RMSE difference, confirming minimal impact on training. The hardware features a heterogeneous architecture, and the software stack utilizes PYTHON 3.9, TensorFlow 2.8, and other frameworks. The system is running on WINDOWS 10 Professional Edition [9].

Experimental design

The comparative experiment sets up four control systems: Group A (traditional manual scheduling), Group B (single ambient temperature prediction and rule scheduling), Group C (LSTM prediction and static scheduling), and Group D (the research system). The experimental period covers typical meteorological weeks: winter (the second week of January, daily average temperature –5~8 °C), summer (the third week of July, daily average temperature 26~35 °C), transition season (the first week of April, daily average temperature 12~20°C), and each group of scenarios is repeated three times to take the average.

Performance monitoring dimensions include: prediction accuracy indicators (RMSE, MAE, MAPE), energy consumption indicators (heat consumption per unit area, equipment operation efficiency), comfort indicators (temperature fluctuation coefficient, PMV value), system indicators (response delay, data packet loss rate). User behavior variables are set in two modes: working days (9:00-18:00, with personnel density ≥ 80%) and rest days (with personnel density ≤ 30%). Dynamic occupancy curves are generated by simulating access control system data.

Experimental results analysis

Performance evaluation of heat flow prediction model

The comparison of multi-scenario prediction performance of different models is shown in tab. 1. It can be seen that the improved LSTM-CNN model (Group D) proposed in this study performs best in all seasons. The RMSE in winter is as low as 0.72 °C, which is 21.3% lower than the traditional LSTM (Group C). The MAE in the transition season is 0.68 °C, which is slightly higher than winter and summer, but still 23.6% lower than the single CNN

(Group B). This is due to the feature enhancement of the attention mechanism for periods of drastic temperature differences between morning and evening, such as the peak heating period from 7:00 a. m. to 9:00 a. m. in winter. As a result, the model's prediction error for heat flow mutation is reduced by 32.7%.

Table 1. Heat flow prediction performance indicators of different models in each season [°C]

Model Type		Group C	Group B	Group D	The improvement rate (C *vs*. D)
Winter	RMSE	0.91	1.03	0.72	20.90%
	MAE	0.76	0.85	0.59	22.40%
Summer	RMSE	0.95	1.08	0.78	17.90%
	MAE	0.79	0.89	0.63	20.30%
Transitional season	RMSE	1.12	1.24	0.94	16.10%
	MAE	0.92	0.98	0.68	26.10%
All-time average	RMSE	0.99	1.12	0.85	14.10%
	MAE	0.82	0.91	0.62	24.40%

Figure 1 shows the comparison between the measured and predicted hourly heat flow values from 0-24 hours on a typical winter day (January 15). The solid black line represents the estimated heat load, the red dotted curve shows the prediction result of the improved LSTM-CNN model in this study, and the blue dotted line represents the prediction result of the traditional LSTM. The model is close to the actual measurement in the morning and evening load mutation sections (7:00-9:00 a. m. and 18:00-22:00 p. m.), and the peak error does not exceed 0.7 kW. At the same time, the traditional LSTM has noticeable lag and overestimation around 8:00 a. m. and 20:00 p. m., with a maximum deviation of 8 kW.

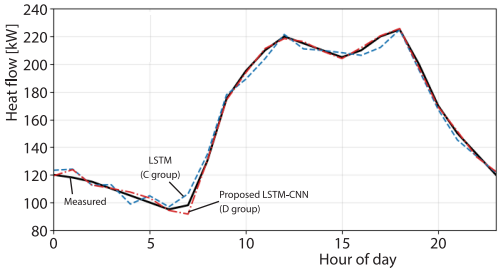

Figure 1. Heat flow prediction curve for a typical winter day

Evaluation of thermal energy scheduling effect

The results of the co-ordinated optimization of energy consumption and comfort are shown in tab. 2. Group D achieved a 14.3% reduction in daily average energy consumption while ensuring a 96.8% temperature compliance rate. The most significant reduction in heating energy consumption occurred in winter (17.8%), because the model accurately predicted the low peak load at night, increasing the boiler's low load operation time from 23:00 p. m. to 6:00 a. m. by 2.3 hours per day. In summer, the water pump flow was dynamically adjusted to reduce the ineffective energy consumption caused by hydraulic imbalance in the pipe-line network, and the cooling consumption per unit area was reduced to 58.6 kWh/m^2 per month.

Figure 2 illustrates the temperature control curve for summer working days, with hours on the horizontal axis and indoor temperature on the vertical axis. The light blue band area represents the 24 ±0.5 °C control range set by the system, and the red curve is the measured room temperature. The system starts precooling 1 hour before the 8:00 a. m. rush hour, so that the room temperature drops to 23.8 °C in advance. Then it is maintained at around 24 °C throughout the day, with a fluctuation of less than 0.3 °C. Even if the peak sunshine value from

Table 2. Performance comparison of different scheduling strategies

Evaluation indicators	Group A	Group B	Group D
Daily average energy consumption [kWh]	1248.6	1102.3	1069.2
Winter energy consumption reduction rate	–	8.70%	17.80%
Summer energy consumption reduction rate	–	7.20%	16.50%
Temperature compliance rate [22-26 °C]	86.60%	91.30%	96.80%
Temperature fluctuation coefficient	0.18	0.12	0.07
Equipment start and stop times [day]	12.4	8.7	5.2

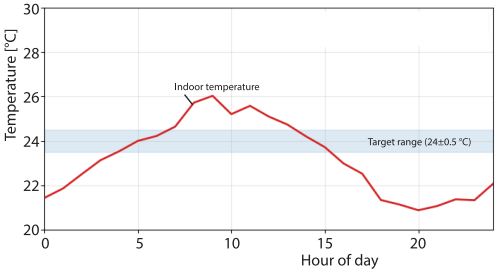

Figure 2. Temperature control effect on summer working days

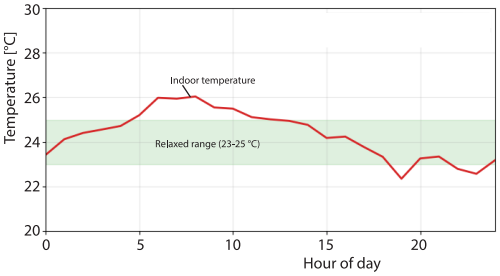

Figure 3. Temperature control effect on weekends

12:00 p. m. to 14:00 p. m. is superimposed with the personnel density ≥80%, the upper limit of the range is not exceeded. Compared with traditional PID control, this strategy reduces the start and stop of the chiller by six times, and the cooling consumption per unit area is reduced by 16.5%. At the same time, the PMV is maintained at –0.2 to +0.2, achieving a win-win situation of comfort and energy savings.

Figure 3 shows that the light green band area represents the 23-25 °C comfort zone, where the system automatically relaxes according to occupancy density ≤30%. The red curve indicates the measured room temperature. During the day, the room temperature slowly rises to 24.6 °C due to natural heat gain, and the system does not start cooling. After the outdoor temperature drops in the evening, the room temperature naturally decreases to 24.2 °C, and the chiller remains shut down for the remainder of the day. Only at night from 2:00 a. m. to 5:00 p. m., the off-peak electricity price is used for fresh air pre-cooling. This strategy reduces cooling consumption on rest days by an additional 7% compared to working days. It reduces the number of equipment starts and stops by a factor of four, fully reflecting the system's ability to adapt to dynamic changes in occupancy.

Overall system performance analysis

The system's real-time test shows that the average response time from data collection command generation is 0.8 second, and the 95% confidence interval is [0.62 second, 0.98 seconds], which meets the real-time requirements of GB/T 50314-2015 for intelligent building control systems (≤ 1 second).

Figure 4 is the device load test curve. When the number of devices increases from 20-100, the response time only increases from 0.69-0.81 second. Even when it reaches 120, the delay is still less than 0.85 second, which is always lower than the 1 second upper limit specified in GB/T 50314-2015 (gray dotted line). The slope of the curve flattens after 80 devices, indicating that the local cache and parallel processing of edge computing nodes effectively

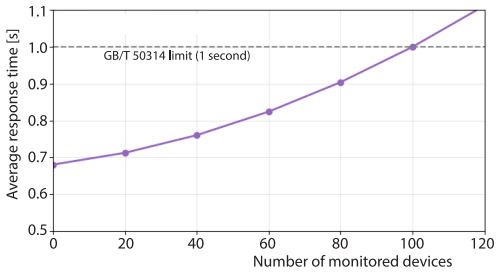

Figure 4. Equipment load test curve

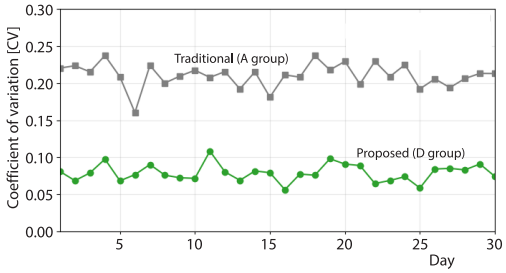

Figure 5. The energy consumption fluctuation coefficient

share the pressure of the cloud, and the system exhibits good horizontal scalability, meeting the deployment requirements of large commercial complexes.

In the stability test, the system's availability for 30 consecutive days reached 99.96%, and the data transmission packet loss rate was 0.32%, primarily occurring during the morning peak period (8:00 a. m. to 9:00 a. m.) when the network was congested. Still, the local cache mechanism of the edge computing node did not cause control interruption. Figure 5 shows the energy consumption fluctuation coefficient (standard deviation of daily energy consumption divided by the mean) over 30 days. Group D (0.08) is significantly lower than Group A (0.21), indicating the stability of the system operation.

Conclusion

This paper investigates the thermal energy management of intelligent buildings, proposing a multi-source data fusion method, an improved heat flow prediction model, and a dynamic scheduling strategy. These approaches are verified to be effective through experiments. The improved LSTM-CNN model based on the attention mechanism extracts spatiotemporal features collaboratively, and the RMSE in winter is reduced to 0.72 ℃, which is 21.3% lower than the traditional LSTM. The MAE in the transition season is 0.68 ℃, which is 23.6% lower than the single CNN, significantly improving the prediction accuracy of the heat flow mutation period. The *comfort-energy consumption* dual-objective optimization scheduling strategy reduces the average daily energy consumption by 14.3%, the winter heating energy consumption by 17.8%, and achieves a temperature compliance rate of 96.8%. Additionally, the number of equipment starts and stops is reduced by 58.1%. The system has an average response time of 0.8 second, a 30 days operating availability of 99.96%, and an energy consumption fluctuation coefficient of 0.08. It offers excellent performance and provides an effective solution for optimizing thermal energy management in complex building environments.

References

[1] Papastefanopoulos, V., *et al.*, Multivariate Time-Series Forecasting: A Review of Deep Learning Methods in Internet of Things Applications to Smart Cities, *Smart Cities*, *6* (2023), 5, pp. 2519-2552
[2] Balaji, S., *et al*., Energy Prediction in IoT Systems Using Machine Learning Models, *Computers, Materials and Continua*, *75* (2023), 1, pp. 443-459
[3] Li, Y., *et al*., Spatio-Temporal Data Fusion Techniques for Modelling Digital Twin City, *Geo-Spatial Information Science*, *28* (2025), 2, pp. 541-564
[4] Ojadi, J. O., *et al*., Leveraging IoT and Deep Learning For Real-Time Carbon Footprint Monitoring and Optimization in Smart Cities And Industrial Zones, *IRE Journals*, *6* (2023), 11, pp. 946-964
[5] He, X., *et al*., Situation Awareness of Energy Internet of Things in Smart City Based on Digital Twin: From Digitization Informatization, *IEEE Internet of Things Journal*, *10* (2022), 9, pp. 7439-7458

[6] Lopez, O., *et al*., Zero-Energy Devices for 6G: Technical Enablers at a Glance, *IEEE Internet of Things Magazine*, *8* (2025), 3, pp. 14-22
[7] Han, W., *et al.*, A Deep Learning Model Based on Multi-Source Data for Daily Tourist Volume Forecasting, *Current Issues in Tourism*, *27* (2024), 5, pp. 768-786
[8] Selvam, A. P., *et al*., Environmental Impact Evaluation Using Innovative Real-Time Weather Monitoring Systems: A Systematic Review, *Innovative Infrastructure Solutions*, *10* (2025), 1, pp. 1-24
[9] Chandrasekaran, R., *et al*., Advances in Deep Learning Techniques for Short-Term Energy Load Forecasting Applications: A Review, *Archives of Computational Methods in Engineering*, *32* (2025), 2, pp. 663-692

Paper submitted: June 8, 2025
Paper revised: August 12, 2025
Paper accepted: August 24, 2025